Osteoarthritis and Cartilage 21 (2013) S63–S312

Osteoarthritis and Cartilage

Poster Presentations OARSI Supplement 2013

100
AGEING AND OSTEOARTHRITIS MARKERS IDENTIFIED BY MALDI IMAGING MASS SPECTROMETRY

M.J. Peffers[†], B. Cillero-Pastor[‡], G. Eijkel[‡], P.D. Clegg[†], R.M. Heeren[‡]. [†]*Univ. of Liverpool, Neston, United Kingdom;* [‡]*FOM Inst. AMOLF, Amsterdam, The Netherlands*

Purpose: Cartilage protein distribution and the changes that occur in cartilage ageing and disease are essential in understanding the process of cartilage ageing and age-related diseases such as osteoarthritis (OA). Matrix assisted laser desorption ionization (MALDI) imaging mass spectrometry (IMS) enables examination of proteins *in-situ* at a high spatial resolution. This study utilised this methodology to investigate the location and abundance of different cartilage proteins in ageing and OA equine cartilage in order to determine changing molecular events distinct between aging and disease.
Methods: For age-related studies samples were taken from skeletally mature young and old horses. For OA studies skeletally mature donors were chosen with mild macroscopic OA changes. 12 μm thick sections were cut in duplicate. Following washing trypsin for digestion was applied and Alpha-Cyano-4-hydroxycinnamic acid matrix deposited. Synapt HDMS MALDI-Q-TOF was used to perform the IMS experiments. Peptides were identified using MASCOT following MS/MS experiments. Biomap software was used to generate ion images and quantify peptide intensity. The data analysis workflow used Principal Component Analysis (PCA) and Discriminant Analysis (DA) for data interpretation. Following IMS samples were stained with haematoxylin and eosin and histologically assessed.
Results: Histological assessment revealed mild changes in the OA samples alone. Protein profiling experiments directly from the tissue sections identified extracellular matrix proteins including cartilage oligomeric matrix protein, fibromodulin, biglycan and type II collagen. After combining all the spectra from the different conditions and following DA, the resulting discriminant functions classified the data in three groups according to their peptide profile: young, old and OA. Interestingly there was a large contribution of the old samples to the negative part of DF1 indicating that peptides within old samples were also present in OA samples. The spectra of young, old and OA samples after MALDI-IMS experiments were analyzed independently by PCA and DA to classify peptides specific to each group (young versus old and old versus OA), thus producing a catalogue of peptides distinct in ageing and disease. Then protein distribution differences were visualised and semi-quantified, through the examination of peptide intensities in young, old and OA cartilage Biomap. A number of OA and ageing markers were identified. Significant differences were evident for the peak intensity distribution of OA specific peptides including fibronectin peptides *m/z* 1349.6 and *m/z* 1401.7 ($p=0.018$, $p=0.02$) and the hypothetical marker with *m/z* 1366.5 ($p=0.001$) between ageing and OA samples. Age-related markers were also identified for COMP *m/z* 2256.1, the hypothetical marker *m/z* 2415.9 and fibromodulin peptide ELHLDHNQISR; *m/z* 1361.7 Furthermore there was a significant reduction in the intensity of this latter peptide (Figure 1) and biglycan peptide NHLVEIPPNLPSSLVELR *m/z* 2027.2 ($p=0.001$, $p=0.02$) in OA (C) compared to young (A) and old (B) cartilage indicating peptides potentially targeted for degradation in OA.

Conclusions: MALDI-IMS based molecular imaging provided a novel platform to study cartilage ageing and disease enabling age and disease specific markers in cartilage to be elucidated and spatially resolved as well as identifying peptides targeted in early OA degradation.

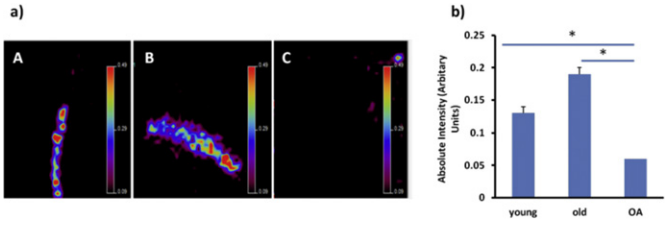

101
GLUCOCORTICOIDS INDUCE SENESCENCE IN PRIMARY HUMAN TENOCYTES: IN VITRO AND IN VIVO EVIDENCE

R.C. Poulsen, A.C. Watts, R.J. Murphy, A.J. Carr, P.A. Hulley. *Univ. of Oxford, Oxford, United Kingdom*

Synthetic glucocorticoids (GCs) are frequently used to treat painful and inflamed tissues and joints. However GCs also cause unwanted side effects, inhibiting cell proliferation as well as normal cell activity. Whether these effects are transient or long-term is unknown. Inhibition of cell proliferation can lead to either quiescence or senescence. Whereas quiescence is reversible, senescence is irreversible in vivo and hence leads to a permanent loss of normal cell functionality.
Purpose: The aim of this study was to determine whether GCs induce senescence in human tenocytes in vitro and in vivo.
Methods: Characteristic features of cell senescence (β-galactsidase activity at pH6 (SA-β-gal), active mTOR in cells in cycle arrest) were examined in GC-treated primary human tenocytes. The effect of GCs on activity of the two main pathways leading to cell senescence (p38/p16INK4a and p53/p21cip) was determined by Western blotting. Gene expression changes were assessed by RT-qPCR. Tendon biopsies were taken from tendinopathy patients immediately prior to and seven-weeks following GC injection. Markers of senescence were analysed in biopsy specimens by immunohistochemistry.
Results: GC treatment of human tenocytes in vitro resulted in a higher percentage of SA-β-gal positive cells. mTOR remained active despite cell cycle arrest in GC-treated tenocytes. Increased p53 acetylation and reduced levels of the p53 deacetylase sirtuin 1 were observed in GC-treated tenocytes. Levels of p21cip, an anti-apoptosis/pro-senescence modulator of p53 activity were also increased post-GC treatment. Knockdown of p53 using RNAi or chemical inhibition of p53 activity prevented GC-induced senescence. Preclusion of the GC-induced reduction in sirtuin 1 levels either by adenoviral-mediated overexpression of exogenous sirtuin 1 or by upregulation of endogenous sirtuin 1 expression by glucose restriction (to emulate caloric restriction) or treatment with resveratrol also prevented GC-induced

senescence. We have previously reported a significant reduction in the percentage of proliferating cells, but no significant change in the percentage of apoptosing cells, in tissue biopsies taken from tendinopathy patients seven weeks after local GC injection compared to in biopsies taken from the same patients immediately prior to injection. In the present study we found the percentage of p53-positive cells in tissue biopsies was significantly higher ($p=0.03$) post-GC injection compared to pre-GC injection. The percentage of p21-positive cells also tended to be higher ($p=0.06$) post-GC injection compared to pre-injection.

Conclusions: Results from this study demonstrate GCs activate the p53/p21 senescence-inducing pathway in vitro and provide compelling evidence that this pathway is also activated following local GC injection in vivo. The loss of normal cell functionality associated with senescence has been linked with disease and degeneration in a number of different tissues. Given the apparent irreversible nature of the senescent phenotype, GC-induced senescence is likely to have long-term detrimental consequences on tissue. The fact that we observed a marked increase in p53 expression seven weeks following GC injection supports the notion that the effects of local GC injection on tendon tissue are not transient. Senescence induction by GCs may exacerbate the underlying tissue pathology responsible for the pain for which the GCs were prescribed to treat.

102
EFFECT OF LONG-TERM VOLUNTARY EXERCISE ON THE INDUCTION OF OSTEOARTHRITIS BY A VERY HIGH-FAT DIET IN AGED MICE

E.E. Hutchison, J. Hudson, G. Roach, T. Griffin. *Oklahoma Med. Res. Fndn., Oklahoma City, OK, USA*

Purpose: Short-term voluntary exercise protects against cartilage proteoglycan loss in young mice fed a very high-fat diet. Exercise also reduces the clustering of metabolic inflammatory markers and improves glucose metabolism without weight loss, suggesting a role for systemic metabolic factors in mediating obesity-associated knee OA. We hypothesized that despite an increase in joint loading, long-term exercise would protect against knee OA in aged mice fed a very high-fat diet by reducing age and diet-associated increases in weight and glucose intolerance.

Methods: Male C57BL/6J mice were fed either a control fat (CF; 10% kcal fat; n=21) or a very high fat (HF; 60% kcal fat; n=22) diet starting at 6 wks of age. At 26 wks, mice from each diet (n=9) were single-housed in cages with a running wheel until the end of the study at 52 wks of age. We compared joint loading between CF and HF fed mice using a custom force-instrumented running wheel. Body composition was quantified by DEXA and dissection of fat pads. Glucose tolerance testing was conducted at 24 and 48 wks. We evaluated OA pathology by MicroCT and histomorphometry. MicroCT was used to evaluate subchondral bone thickness and relative trabecular bone volume (BV/TV) in the medial and lateral tibial compartments. Stained sagittal knee sections were graded for cartilage OA severity using a modified Mankin scale (0-24), and anterior and posterior medial tibial osteophytes were graded using a semi-quantitative scale (0-3) by two blinded graders.

Results: Prior to exercise, body weight and body fat were increased 71% and 63%, respectively, with HF feeding. Voluntary running distance (7.1 vs. 2.7 km/day), speed (59 vs. 33 cm/s) and peak limb force (115 vs. 92 % bodyweight) were lower in HF fed animals ($p<0.05$). Exercise did not significantly decrease body weight or epididymal fat pad mass in HF animals, although weight and fat mass were reduced with exercise in CF animals (Fig. 1A, B). Glucose tolerance area under the curve (AUC) was greater in exercised but not sedentary HF fed animals compared to activity-matched dietary controls (Fig 1C). A HF diet increased cartilage OA scores in both activity groups (Fig. 2A, $p=0.007$), although there was no effect of exercise. There was, however, a trend for decreased osteophyte formation in exercised animals regardless of diet (Fig. 2B, $p=0.05$).

Conclusions: Contrary to our hypothesis, long-term voluntary wheel running exercise did not protect against HF diet-induced obesity, glucose intolerance, or OA severity in aged mice. Unlike short-term exercise in young HF-fed mice, mice that have already developed substantial diet-induced obesity show a decreased propensity for long-term voluntary wheel running exercise, which may contribute to the minimal activity-dependent changes with HF feeding in this study. Increased OA severity with long-term HF feeding was primarily due to increased cartilage degradation and proteoglycan loss and not due to increased osteophyte formation. Future work is needed to determine if systemic inflammatory markers are reduced with exercise in CF or HF fed animals to better understand the relationship between systemic metabolic inflammation and OA pathology.

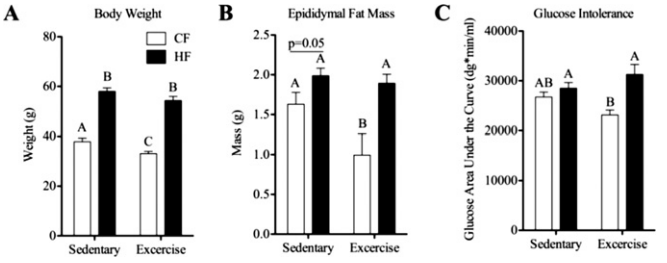

Figure 1. Effect of a HF diet and long-term exercise on body weight, epididymal fat mass, and glucose intolerance in 52-wk old mice. Bars sharing the same letters arc not significantly different from each other ($p>0.05$).

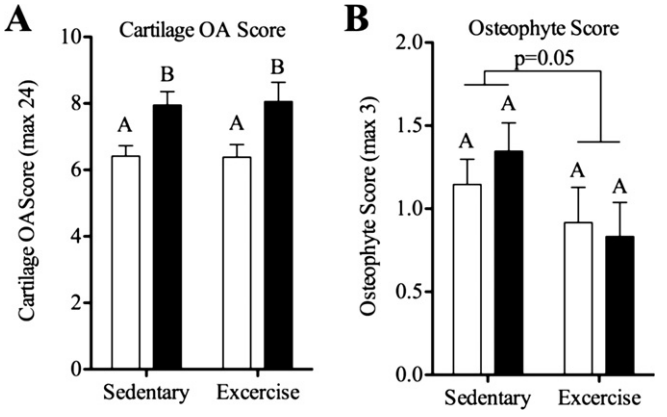

Figure 2. Effect of a HF diet (filled bars) and long-term exercise on OA severity in 52-wk old mice. Bars sharing the same letters are not significantly different from each other ($p>0.05$).

103
EARLY RESPONSES OF JOINT TISSUES TO NONINVASIVE MOUSE KNEE INJURY PROVIDE POTENTIAL TARGETS FOR THERAPY

P. Wu [†,‡], N. Holguin [†], M.J. Silva [†], W. Liao [‡], L.J. Sandell [†]. [†] *Washington Univ. Sch. of Med., Saint Louis, MO, USA;* [‡] *The First Affiliated Hosp. of Sun Yat-sen Univ., Guangzhou, China*

Purpose: Joint trauma can lead to a spectrum of acute lesions, including articular cartilage degradation, ligament or meniscus tears, synovitis, and osteophyte formation, all potentially associated with osteoarthritis. The events induced by over loading of the knee are poorly defined. The goal of this study was to generate and validate a murine model of non-invasive knee joint trauma following controlled injurious compression in vivo.

Methods: Animals experienced normal locomotion, except during loading. Loading was applied non-invasively via axial compression of the mouse lower leg, with points of contact at the distal femur and foot. This results in compressive joint loading across the femoro-tibial joint. The right knee of mice was subjected to one of three peak forces (3, 6, 9 N) in axial compression for 60 cycles (0.3 sec of load/unload followed by 10 sec of rest) for 1 day and harvested at 5, 9 and 14 days post loading (n=3-5 for each time point). The left knee was not loaded and served as the contralateral control. Histological and immunohistochemical analyses were performed to evaluate pathologic features in posttraumatic joint tissues.